THE JOURNAL OF BIOLOGICAL CHEMISTRY VOL. 287, NO. 26, pp. 21992–22003, June 22, 2012
© 2012 by The American Society for Biochemistry and Molecular Biology, Inc. Published in the U.S.A.

Highly Potent Inhibitors of Proprotein Convertase Furin as Potential Drugs for Treatment of Infectious Diseases*[S]

Received for publication, December 12, 2011, and in revised form, April 19, 2012 Published, JBC Papers in Press, April 26, 2012, DOI 10.1074/jbc.M111.332643

Gero L. Becker[‡1], **Yinghui Lu**[§1,2], **Kornelia Hardes**[‡], **Boris Strehlow**[¶], **Christine Levesque**[‖3], **Iris Lindberg**[**], **Kirsten Sandvig**[‡‡], **Udo Bakowsky**[¶], **Robert Day**[‖], **Wolfgang Garten**[§4], **and Torsten Steinmetzer**[‡5]

From the [‡]*Institute of Pharmaceutical Chemistry,* [§]*Institute of Virology, and* [¶]*Institute of Pharmaceutical Technology and Biopharmacy, Philipps University, 35032 Marburg, Germany, the* [‖]*Institut de Pharmacologie de Sherbrooke, University of Sherbrooke, Sherbrooke, Quebec J1H SN4, Canada, the* [**]*Department of Anatomy and Neurobiology, University of Maryland, Baltimore, Maryland 21201, and the* [‡‡]*Department of Biochemistry and Centre for Cancer Biomedicine, Institute for Cancer Research, Norwegian Radium Hospital, Montebello, 0310 Oslo, Norway*

Background: Furin and furin-like proprotein convertases are involved in disease-related processes and have emerged as potential drug targets.
Results: The incorporation of basic acyl residues at P5 position provides highly potent inhibitors of furin, PC1/3, PC4, PACE4, and PC5/6.
Conclusion: These inhibitors could be potential drugs for the treatment of infectious diseases.
Significance: The most potent synthetic inhibitors of furin-like proprotein convertases have been developed.

Optimization of our previously described peptidomimetic furin inhibitors was performed and yielded several analogs with a significantly improved activity. The most potent compounds containing an N-terminal 4- or 3-(guanidinomethyl)phenylacetyl residue inhibit furin with K_i values of 16 and 8 pM, respectively. These analogs inhibit other proprotein convertases, such as PC1/3, PC4, PACE4, and PC5/6, with similar potency, whereas PC2, PC7, and trypsin-like serine proteases are poorly affected. Incubation of selected compounds with Madin-Darby canine kidney cells over a period of 96 h revealed that they exhibit great stability, making them suitable candidates for further studies in cell culture. Two of the most potent derivatives were used to inhibit the hemagglutinin cleavage and viral propagation of a highly pathogenic avian H7N1 influenza virus strain. The treatment with inhibitor 24 (4-(guanidinomethyl)phenylacetyl-Arg-Val-Arg-4-amidinobenzylamide) resulted in significantly delayed virus propagation compared with an inhibitor-free control. The same analog was also effective in inhibiting Shiga toxin activation in HEp-2 cells. This antiviral effect, as well as the protective effect against a bacterial toxin, suggests that inhibitors of furin or furin-like proprotein convertases could represent promising lead structures for future drug development, in particular for the treatment of infectious diseases.

Furin, the translational product of the *fur* gene, was discovered in 1986 (1). Because of its homology with the Kex2 prohormone processing serine protease from *Saccharomyces cerevisiae*, furin was identified as the first member of the family of secretory proprotein convertases (PC)[6] in humans, all of which contain a subtilisin-like protease domain (2, 3). Nine human PCs have now been identified. Two of these, SKI-1 and PCSK9, cleave their substrates after paired hydrophobic amino acid residues, such as leucine or isoleucine, whereas the other seven classical PCs (furin, PC2, PC1/3, PACE4, PC4, PC5/6, and PC7) strictly require a basic amino acid as a P1 residue (4, 5).

Furin is ubiquitously expressed as type I transmembrane protein and is present both in vertebrates and invertebrates. The protein is mainly located in the Golgi and trans-Golgi network but may also circulate through the endosomal system to the cell surface and back to the trans-Golgi network, and it is partially shed as a soluble, truncated enzymatically active enzyme (6–8). Furin catalyzes the physiological activation of proforms of receptors, hormones, zymogens, and cell surface proteins (9). It has a more rigid preference for a basic amino acid in the P2 position than other furin-like PCs, leading to its preferred consensus sequence Arg-Xaa-(Lys/Arg)-Arg ↓ -Xaa, where bulky hydrophobic residues in P1′ position are unfavorable (10, 11). A study of furin-deficient mice demonstrated the importance of this enzyme during embryogenesis; the knock-out of the *fur* gene led to an early death at embryogenic day 11 due to the failure of ventral closure and embryonic turning (12). However,

* This work was supported in part by National Institutes of Health Grant DA05084 (to I. L.). This work was supported in part by the Ministère du Développement Économique, Innovation et Exportation, and Canadian Institutes of Health Research (to R. D.).
[S] This article contains supplemental Figs. S1–S7, Table S1, and additional references.
[1] Both authors contributed equally to this work.
[2] Supported by the Landesoffensive zur Entwicklung Wissenschaftlich-Ökonomischer Exzellenz des Landes Hessen, the Roland and Elfriede Schauer-Stiftung, and the FAZIT-Stiftung.
[3] Supported by Fonds de Recherche du Québec-Santé studentship.
[4] Supported by Deutsche Forschungsgemeinschaft SFB 593.
[5] To whom correspondence should be addressed: Institute of Pharmaceutical Chemistry, Philipps University, Marbacher Weg 6, D-35032 Marburg, Germany. Tel.: 49-6421-2825900; Fax: 49-6421-2825901; E-mail: steinmetzer@staff.uni-marburg.de.

[6] The abbreviations used are: PC, proprotein convertase; MDCK, Madin-Darby canine kidney cell; FPV, fowl plague virus; CMK, chloromethyl ketone; Dec-, decanoyl-; Amba, amidinobenzylamide; Fmoc, *N*-(9-fluorenyl)methoxycarbonyl; Boc, *t*-butoxycarbonyl; AMC, 7-amido-4-methylcoumarin; RFU, relative fluorescence unit.

studies with furin-deficient cell lines (13) and a liver-specific interferon-inducible knock-out mouse showed no obvious adverse effects implying that other PCs may be able to compensate for furin deficiency due to partly overlapping expression patterns and subcellular localizations (14, 15). In addition to its normal physiological role, furin contributes to the maturation of many disease-related proteins and is involved in viral and bacterial infections, tumorigenesis, neurodegenerative disorders, diabetes, or atherosclerosis (7, 16, 17). For example, many viruses contain fusogenic surface glycoproteins that must be cleaved by furin or a furin-like PC as a prerequisite for virus propagation. Among these are the hemagglutinins (HA) of H5 and H7 subtypes of the highly pathogenic avian influenza viruses that cause bird flu and the surface glycoproteins of the HIV, Ebola, Marburg, and measles viruses (7, 18, 19). In addition, furin is involved in various bacterial infections. It processes the protective antigen precursor of *Bacillus anthracis*, a component of anthrax toxin; it also cleaves *Pseudomonas* exotoxin, Shiga toxin, Shiga-like toxins, and diphtheria toxin, thereby contributing to their pathogenicity (7). Also among its substrates are growth factors, matrix metalloproteases, and adhesion molecules, all of which are important for tumor progression and malignancy (20, 21). Because of its involvement in many disease-related processes, furin has emerged as a potential drug target.

The first furin inhibitors were based on irreversibly inhibiting chloromethyl ketones (CMKs) (18, 22). Several other inhibitor types were later designed (23). In addition to macromolecular compounds, such as α_1-antitrypsin Portland (24), mutated forms of eglin c (25), and the synthetic complete 83-mer prodomain of furin (26), various types of oligopeptidic and small molecule inhibitors have also been prepared. Certain peptide inhibitors were derived from either substrate sequences (27) or from the furin prodomain (28), or they were identified by screening of peptide libraries (29). A strong inhibitory activity was found for polyarginines, such as nona-D-arginine, which inhibits furin with a K_i value of 1.3 nM (30). By contrast, most nonpeptide small molecules possess only moderate activity in the micromolar range (23, 31, 32). An exception is the series of potent tetrabasic 2,5-dideoxystreptamine derivatives, one of which inhibits furin with a K_i value of 6 nM (33).

Recently, we have developed a series of reversible competitive substrate analog furin inhibitors containing decarboxylated arginine mimetics in the P1 position (34). Phenylacetyl-Arg-Val-Arg-4-amidinobenzylamide (compound **1**) possesses a K_i value of 0.81 nM and has a similar potency against PC1/3, PACE4, and PC5/6, whereas PC2, PC7, and several trypsin-like serine proteases were poorly inhibited. Modification of the P3 position provided several compounds with similar potency, whereas the replacement of the P4 Arg residue or the incorporation of amino acids in D-configuration was not accepted (35). Despite its excellent activity *in vitro*, compound **1** showed reduced potency in a cellular assay as an inhibitor of the cleavage of the fowl plague hemagglutinin of the subtype H7, possessing a multibasic furin cleavage site. We assumed that this might be related to limited accessibility of these inhibitors to their intracellularly located target, furin.

To improve the cellular performance of these inhibitors, we have synthesized new analogs derived from our lead structure **1**. Examination of the x-ray structure of mouse furin covalently bound to the irreversible substrate analog inhibitor decanoyl-Arg-Val-Lys-Arg-CMK revealed that its P5 residue is directed into the solvent and might be a suitable residue for further optimization (36). In a first approach, based on results obtained during the development of the initial decanoylated chloromethyl ketone inhibitor (22, 37) and recent reports regarding the improved membrane permeability of octaarginine after acylation with a hexanoyl residue (38), we have incorporated saturated and unsaturated fatty acid residues in the P5 position. In a second approach, the linear acyl groups were replaced by hydrophobic cyclic residues; and in a third series, we modified the inhibitors with various basic P5 groups. In this study, we describe the synthesis and characterization of these new furin inhibitors. The most potent analogs were examined for their ability to block both fowl plague virus (FPV) propagation and activation of Shiga toxin. Our successful use of these new furin inhibitors suggests broad therapeutic potential.

EXPERIMENTAL PROCEDURES

Information regarding the reagents used for synthesis and analytical methods for inhibitor characterization are provided in the supplemental material.

Synthesis of Inhibitors—The inhibitors were synthesized by a combination of solid phase peptide synthesis and solution synthesis, as described previously (34, 35). Briefly, the P2-P5 segments were synthesized by Fmoc strategy on acid-labile 2-chlorotrityl chloride resin, which allowed the mild cleavage of the intermediates from the resin under side chain protection. After coupling of the unprotected P1 4-amidinobenzylamine in solution, all protecting groups were removed, and the inhibitors were purified by preparative reverse phase HPLC and obtained as lyophilized trifluoroacetic acid (TFA) salts. In case of inhibitors **20**, **22**, **24**, **26**, and **28,** a final guanylation was performed by treatment of the amine precursors with 1*H*-pyrazole-1-carboxamidine (39). As an example, the synthesis strategy of the most potent inhibitor **26** and its amine precursor **25** is shown in Scheme 1.

Enzyme Kinetics with Furin—The inhibition constants of inhibitors **1**-**9** and **12**-**18** (Table 1) were determined with recombinant soluble human furin (30) at room temperature according to the method of Dixon (40) using the fluorescence plate reader Safire 2 (Tecan, Switzerland) at λ_{ex} = 380 nm, λ_{em} = 460 nm and pyroglutamyl-Arg-Thr-Lys-Arg-AMC as substrate (Bachem, Switzerland) in 100 mM HEPES buffer, pH 7.0, containing 0.2% Triton X-100, 2 mM $CaCl_2$, 0.02% sodium azide, and 1 mg/ml BSA, as described previously (34). The lowest inhibitor concentration used was at least 10 times higher than the enzyme concentration in the assay to avoid tight binding conditions.

The kinetic analysis of inhibitors **10** and **11** revealed nonlinear curves in the Dixon plot (Fig. 1); therefore, only IC_{50} values could be obtained for both compounds. Only for the purpose of comparison, additional IC_{50} values were also determined for certain other inhibitors (**7**, **12**-**14**), although for these analogs

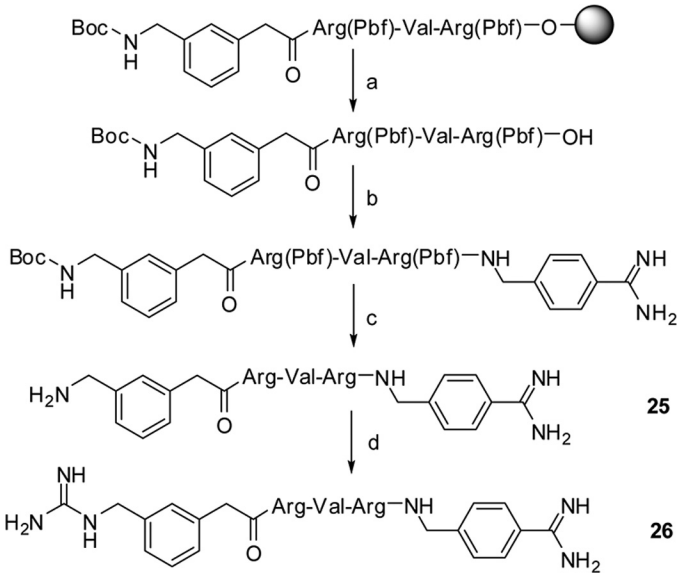

SCHEME 1. **Synthesis of inhibitors 25 and 26.** The N-terminal Boc-protected P5-P2 segment was prepared on a 2-chlorotrityl chloride resin using 3-(Boc-aminomethyl)phenylacetic acid for the coupling of the P5 group and otherwise using a standard Fmoc protocol. *a,* cleavage from resin with 1% TFA in DCM, two times for 30 min, drying *in vacuo*; *b,* 1.5 eq 4-aminomethylbenzamidine·2 HCl, 1.7 eq PyBOP, 4.5 eq 6-Cl-1-hydroxybenzotriazole, 10 eq DIPEA in DMF, 2 h; *c,* TFA/TIS/H_2O (95:2.5:2.5, v/v/v), 3 h at 35 °C, precipitation in cold diethyl ether, preparative reversed phase HPLC; *d,* 5 eq 1*H*-pyrazole-1-carboxamidine·HCl in 1 M Na_2CO_3, 24 h, purification by preparative HPLC. *DCM*, dichloromethane; *PyBOP*, benzotriazol-1-yl-*N*-oxy-tris(pyrrolidino)-phosphonium hexafluorophosphate; *DIPEA*, diisopropylethylamine; *DMF*, *N,N*-dimethylformamide; *TIS*, triisopropylsilane.

K_i values were obtainable. The v, I data pairs of the IC_{50} curves (Fig. 2) were fitted to the three-parameter Equation 1, where v is the steady-state velocity at different inhibitor concentrations; v_0 is the constant velocity in absence of inhibitor; I is the inhibitor concentration, and s is a slope factor.

$$v = \frac{v_0}{1 + \left(\frac{I}{IC_{50}}\right)^s} \quad \text{(Eq. 1)}$$

The v and I data pairs of the tight binding inhibitors **19**-**28** were fitted to Equation 2 (41),

$$v = v_0 \cdot \frac{[(K_i^* + I - E)^2 + 4K_i^* \cdot E]^{1/2} - (K_i^* + I - E)}{2 \cdot E} \quad \text{(Eq. 2)}$$

where v_0 is the constant velocity in absence of inhibitor; I and E are the inhibitor and enzyme concentrations, and K_i^* is an apparent inhibition constant at the substrate concentration used. The true K_i values were calculated from these apparent inhibition constants using Equation 3.

$$K_i = \frac{K_i^*}{1 + \left(\frac{S}{K_m}\right)} \quad \text{(Eq. 3)}$$

Information on enzyme kinetic studies with the other PCs is given in the supplemental Table S1.

TABLE 1
Inhibition of furin by inhibitors of the general formula

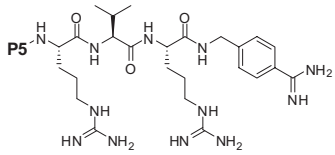

No.	P5	HPLC (min)	MS calc.	MS found[a,b]	K_i (nM)	IC_{50} (nM)
1	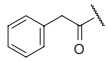	24.2	678.41	679.4[a]	0.81	nd[e]
2		15.12	560.37	281.21[b]	7.6	33
3		16.83	602.38	302.25[b]	1.0	nd[e]
4		20.40	630.41	316.26[b]	0.67	nd[e]
5		26.29	658.44	330.30[b]	0.78	nd[e]
6		32.73	686.47	344.29[b]	0.67	2.3
7		38.78	714.5	358.32[b]	1.6	8.3
8		15.16[c]	742.53	372.32[b]	5.6	nd[e]
9		20.40[c]	770.56	386.37[b]	50	396
10		25.38[c]	798.6	400.37[b]	nd[e]	80
11		30.66[c]	826.63	414.49[b]	nd[e]	14010
12	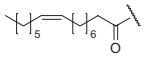	54.50	796.58	399.80[b]	nd[e]	289
13	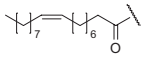	58.20	824.61	413.63[b]	nd[e]	272
14	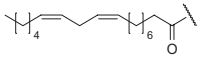	55.10	822.6	412.56[b]	5.3	22
15	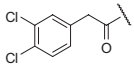	31.72	746.33	374.24[b]	1.2	nd[e]
16	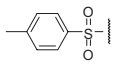	27.02	714.37	358.25[b]	5.3	nd[e]
17	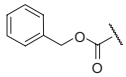	27.78	694.4	348.27[b]	2.4	nd[e]
18	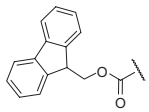	36.80	782.43	329.31[b]	8.5	nd[e]
19	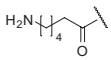	16.50	673.45	337.88[b]	0.096[d]	nd[e]

TABLE 1—*continued*

20	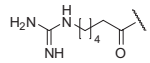	19.30	715.47	358.88[b]	0.085[d]	nd[e]
21	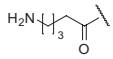	15.70	659.43	330.91[b]	0.070[d]	nd[e]
22	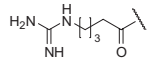	17.30	701.46	351.88[b]	0.062[d]	nd[e]
23	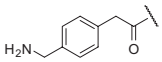	18.10	707.43	354.89[b]	0.033[d]	nd[e]
24	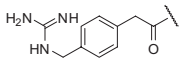	19.70	749.46	375.91[b]	0.016[d]	nd[e]
25	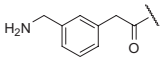	19.48	707.43	354.73[b]	0.037[d]	nd[e]
26	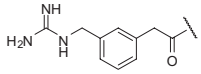	20.41	749.46	750.38[a]	0.008[d]	nd[e]
27	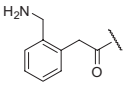	19.50	707.43	708.5[a]	0.127[d]	nd[e]
28	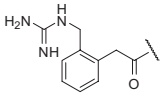	21.50	749.46	750.5[a]	0.291[d]	nd[e]

[a] $(M + H)^+$.
[b] $(M + 2H)^{2+}/2$.
[c] The HPLC starting condition was 30% acetonitrile containing 0.1% TFA, and all other HPLC measurements started at 1% acetonitrile (see supplemental material).
[d] K_i values were determined under tight-binding conditions.
[e] nd means not determined.

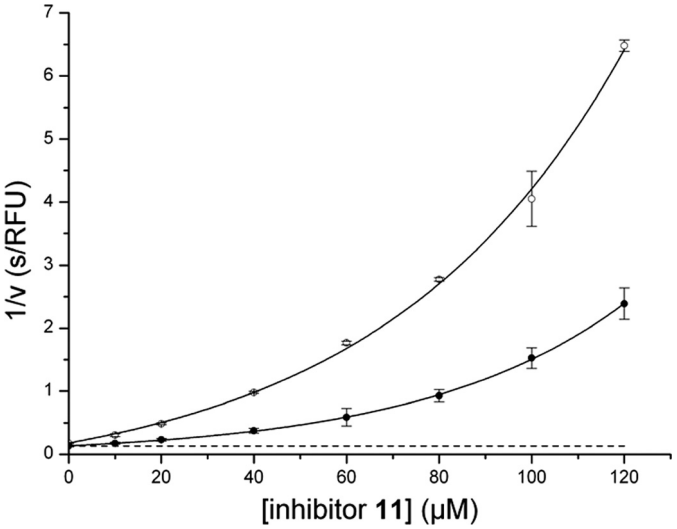

FIGURE 1. **Dixon plot for the stearoyl inhibitor 11, the shown data are the means ± S.E. of three independent measurements.** The nonlinear curves (substrate concentrations 32.5 (●) and 13 (○) μM) do not permit the calculation of a true K_i value according to a classical competitive mechanism. Only for the purpose of better visualization, the data points have here been connected by fitting to an exponential growth curve. The *dashed line* parallel to the *x* axis represents $1/V_{max}$.

Size Measurements of Inhibitor Assemblies—To detect micelle formation of analogs with long acyl residues in the P5 position, light scattering measurements were performed by photon correlation spectroscopy using a Zetasizer Nano ZS (Malvern Instruments, Herrenberg, Germany) equipped with a 10-milliwatt HeNe laser at a wavelength of 633 nm at 25 °C, as described previously (42). Scattered light was detected at an angle of 173° with laser attenuation, and the measurement position was adjusted automatically by the Malvern software. Values given are the means ± S.D. of three independent experiments with each experiment consisting of three measurements of the same sample with at least 10 runs each, as determined by the instrument (Zetasizer Software 6.01).

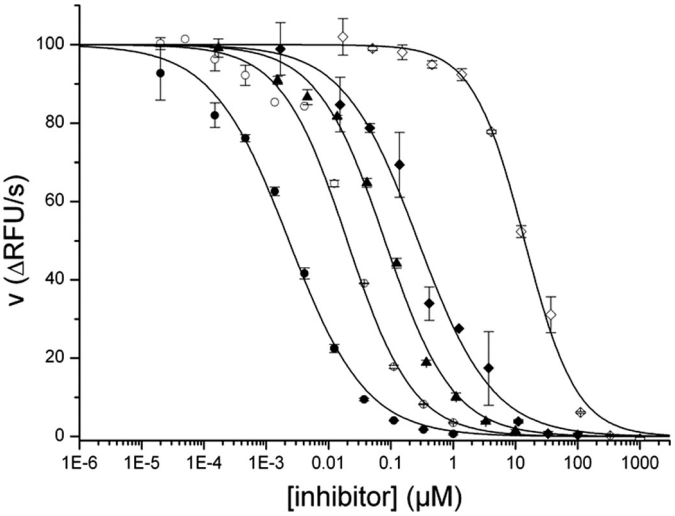

FIGURE 2. **IC_{50} determination for inhibitors 6 (●), 10 (▲), 11 (◇), 13 (◆), and 14 (○).** The shown data are the means ± S.E. of three independent measurements and were performed at a fixed substrate concentration of 8.13 μM. The data were fitted to Equation 1.

Stability Measurements of Inhibitors with HPLC—Stability measurements of inhibitors **22** and **24** were performed by incubating the compounds at 30 or 10 μM final concentrations in Dulbecco's modified Eagle's medium (DMEM) in the presence or absence of MDCK cells under cell culture conditions (37 °C, 5% CO_2, and 80% humidity). At different time points (0, 24, 48, 72, and 96 h), 200 μl of the supernatant were removed and centrifuged (30,000 × *g*, 15 min), and 100 μl were analyzed by analytical reverse phase HPLC; quantitative determination of the inhibitor peak area yielded the amount of inhibitor remaining at each time point.

Inhibition of Hemagglutinin Cleavage and Inhibition of Multiple Cycle Replication of FPV—All information regarding the MDCK cells used, the cell culture conditions, the antiserum for HA cleavage detection, the SDS-PAGE, including Western blot analysis, and the avian influenza virus A/chicken/Rostock/34 (H7N1) has been provided previously (34, 43) and additionally are contained in the supplemental material. Quantitative determination of the infectious virus particles released from cells after multiple cycle replication was performed by a microplaque assay (44).

Inhibition of Shiga Toxin Activation—The [^{3}H]leucine was purchased from Hartman Analytic (Braunschweig, Germany), and the Shiga toxin was a generous gift from Dr. J. E. Brown (United States Army Medical Research Institute of Infectious Diseases, Frederick, MD). The HEp-2 cells used were maintained in DMEM (45). For cytotoxicity assays, cells were seeded into 24-well plates at a density of 5×10^4 cells/well 1 day before

the experiment. The Shiga toxin cytotoxicity assay was performed as described previously (46).

RESULTS

Design and Activity of Inhibitors—All structures, analytical data, IC_{50} and K_i values of the newly synthesized furin inhibitors are summarized in Table 1; data for the previously described inhibitors **1** and **3** are provided for reference.

A comparison of the K_i values determined for inhibitors **2–9** revealed that the P5 residue clearly contributes to binding affinity, because analog **2**, lacking an acyl group, has an ~10-fold reduced activity compared with inhibitors **1** or **3**. In contrast, there were only marginal differences, with inhibition constants close to 1 nM, between compounds **2** and **7**. A gradual loss in inhibitory potency was observed with longer acyl chains possessing more than 10 carbon atoms, *e.g.* for the myristoylated derivative **9** a K_i value of 50 nM was determined. Interestingly, we could not obtain inhibition constants for the palmitoyl and stearoyl inhibitors **10** and **11** due to nonlinear curves in the Dixon plot (see Fig. 1 for inhibitor **11**).

Because of these nonlinear curves in the Dixon plot, only IC_{50} values were determined for both analogs. For comparison, we also used other inhibitors with known K_i values for these IC_{50} measurements (Fig. 2). We assumed that the nonlinear curves in the Dixon plots and reduced potency in IC_{50} measurements of compounds **10** and **11** might be related to a kind of inhibitor assembly or micelle formation. To overcome this problem, related nonsaturated analogs **12**-**14** also containing 16 or 18 carbon atoms were synthesized, because it is known that acyl residues containing *cis*-double bonds are more flexible and exhibit a reduced tendency for micelle formation. For these three inhibitors, linear curves in the Dixon plots were observed, allowing K_i determinations according to a normal competitive reversible mechanism (Table 1). Interestingly, the linoyl derivative **14** (K_i value of 5.3 nM) was significantly more potent than the two analogs containing only one double bond.

To verify the different tendencies of saturated and unsaturated analogs to form micelles, light scattering experiments by photon correlation spectroscopy were performed; we surmised that this could yield better insight into the substructure of liquid formulations. The formation of self-organizing structures such as micelles results in a change in the intensity of scattered light; in addition, the hydrodynamic diameter of the micellar structures can be determined. The tendency of the selected inhibitors to form micelles was investigated in a concentration range from 0.02 to 200 μM. The fluid acetyl-, octanoyl-, and decanoyl (Dec) derivatives **3**, **6** (curve for inhibitor 6 not shown), and **7** showed no concentration-dependent change in scattered light intensity (Fig. 3). A significant increase in signal intensity was, however, observed at concentrations above 200 μM for the decanoyl compound (data not shown). The stearyl, oleoyl, and linoyl derivatives **11**, **13**, and **14**, all possessing 18-carbon atom-long P5 chains, showed a concentration-dependent (stearyl 0.4–0.5 μM, oleoyl 1–1.5 μM, and linoyl 40–50 μM) increase in scattered light intensity, indicating micelle formation. The sizes of the micelles were determined as 468 ± 28.5 nm (stearyl; at 0.5 μM), 324 ± 22.5 nm (oleoyl; at 2 μM), and 330 ± 32.4 nm (linoyl; at 40.0 μM). The mean diameters of the micellar systems also increased with increasing inhibitor concentrations. At the highest concentration investigated (*i.e.* 200 μM), the structures reached diameters of 2,928 ± 431 nm (stearyl, see supplemental Fig. S1), 2,183 ± 377 nm (oleoyl), and 1,478 ± 285 nm (linoyl).

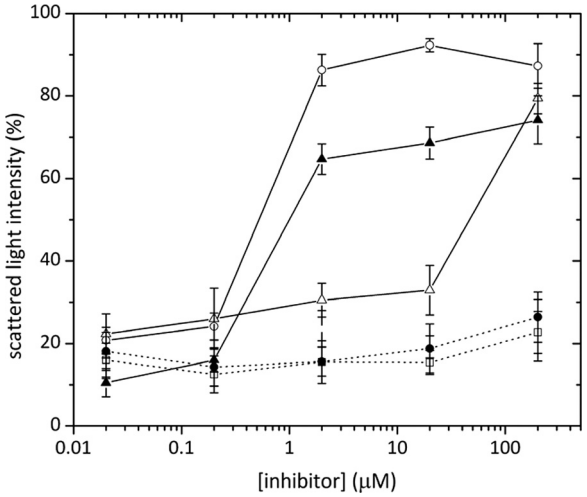

FIGURE 3. **Concentration dependence of light scattering (in %) determined for inhibitors 3 (□), 7 (●), 11 (○), 13 (▲), and 14 (△) in the buffer used for enzyme kinetics.** *Dotted lines* indicated no micelle formation in the concentration range used.

In addition to inhibitors **3**-**14** with linear acyl residues, we also prepared compounds **15**-**18** containing cyclic and relatively hydrophobic P5 groups. These analogs were less potent than our lead **1** and were therefore not further studied. Because various furin substrates contain an additional arginine or lysine residue in the P5 or P6 position (11), a third inhibitor series made by incorporation of basic P5 residues was prepared (compounds **19**-**28**). Significantly improved inhibition was observed with all of these compounds (Table 1). The inhibition constants for these derivatives had to be determined under tight binding conditions, *i.e.* at similar concentrations of enzyme and inhibitor. In contrast to classical inhibitors (used $[I] \gg [E]$), the kinetic analysis of tight binding inhibitors according to Equation 2 requires a knowledge of the active enzyme concentration. Active site titration of serine proteases is normally done with appropriate ester substrates, leading to a rapid formation of an acyl enzyme (47, 48). For furin, active site titration has been described with the amide substrate Boc-Arg-Val-Arg-Arg-AMC, which also shows burst kinetics (49); however, this substrate was not available to us. Other groups have performed active site titration of PCs by incubating enzymes with different concentrations of an irreversible CMK inhibitor around the expected enzyme concentration for a defined time (~30 min) and measuring the residual enzyme activity (24). The resulting plots (Fig. 4) provide the active enzyme concentration as the intersection with the *x* axis. Our attempts to perform this kind of active site titration with the commercially available Dec-Arg-Val-Lys-Arg-CMK in the same buffer as used for enzyme kinetics revealed that a preincubation period of 30 min was not sufficient. In our hands, a stable value of ~1.2 nM for the enzyme concentration was not obtained until after ~2 h of preincubation (Fig. 4, *A* and *B*). Despite correcting for the peptide content of the CMK inhibitor provided by the supplier, this value of 1.2

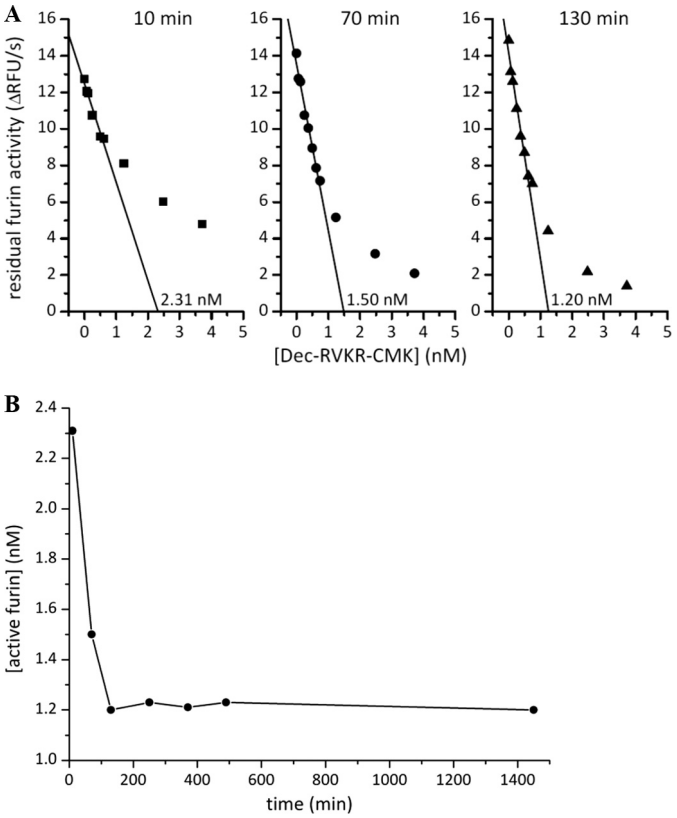

FIGURE 4. **Active site titration attempts of furin using Dec-Arg-Val-Lys-Arg-CMK.** *A,* determination of the remaining enzyme activity after preincubation of furin with different concentrations of the irreversible inhibitor Dec-Arg-Val-Lys-Arg-CMK (times for preincubation indicated in the graphs). *B,* concentration of active furin obtained was dependent on the preincubation time, providing a relatively constant value of ~1.2 nM only after 2 h of preincubation.

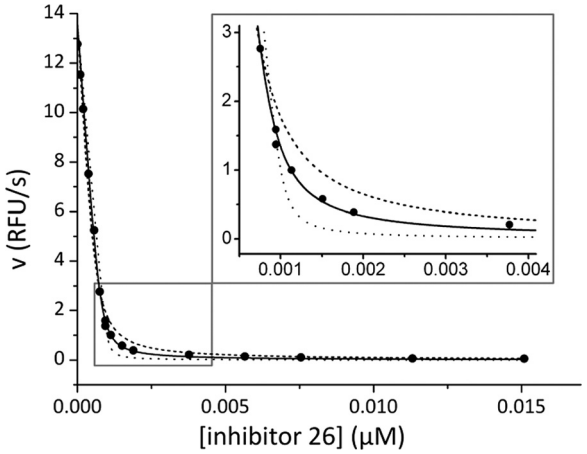

FIGURE 5. **Enzyme kinetic analysis of inhibitor 26 in presence of 8.13 μM substrate.** The measured data were fitted to Equation 2, providing a furin concentration of 0.81 nM as a parameter (*solid line*). In contrast, fits performed using different constant enzyme concentrations were unsatisfactory (*e.g.* furin fixed to a concentration of 1 nM (*dotted line*) and fixed to 0.6 nM (*dashed line*).

nM was slightly higher than the furin concentration of 0.95 nM, calculated based on protein content determination. We assumed that the difference between the titrated furin value and the protein concentration might have arisen from an uncertainty of the true inhibitor concentration, perhaps due to instability of the CMK derivative in the buffer at pH 7.0. Therefore, the stability of the CMK inhibitor in the buffer used for enzyme kinetics was also tested by analytical HPLC. The data could be fitted to a first-order reaction, providing a half-life of ~11.4 h (see supplemental Fig. S2). Therefore, we believe that the active site titration using a CMK inhibitor is influenced by a certain amount of inaccuracy in the concentration of the inhibitor.

To reconcile these different furin concentration values, we used a different approach to determine the concentration of active furin; this approach has been described for the K_i determination of the highly potent thrombin inhibitor hirudin. In this case, the true concentration of the hirudin isolated from leech was unknown, and therefore its concentration was simply modified by an additional parameter during fitting using Equation 2 (50). By analogy, in addition to K_i^*, we used the unknown furin concentration as a second parameter for fitting the v and I data pairs obtained from measurements with the highly potent tight-binding inhibitors to Equation 2. The value of ~0.81 nM obtained (Fig. 5 for inhibitor **26**) was slightly lower than the calculated furin concentration of 0.95 nM determined from the protein content. To confirm the validity of this approach, we attempted to fit the measured data using a slightly higher (1.0 nM) or lower (0.6 nM) fixed enzyme concentration. In both cases, it was impossible to fit the measured data to Equation 2 (Fig. 5, *dotted* and *dashed lines*). To avoid errors in the concentrations of the tight-binding inhibitors **19**-**28** used, their peptide contents were calculated based on the nitrogen content obtained from elemental analysis. These experimentally determined peptide contents were between 90 and 97% of the calculated values in all cases, assuming that one molecule of trifluoroacetic acid is attached as a counter-ion to each basic group in the inhibitor.

Linear progress curves were observed during all kinetic measurements, indicating a reversible inhibition mechanism for all inhibitors. Several compounds containing a basic P5 residue were found to be highly potent tight-binding inhibitors of furin. The most potent analogs **24** and **26**, modified by an N-terminal *p*- or *m*-guanidinomethyl-phenylacetyl group, possess K_i values of 16 and 8 pM, respectively. Selected inhibitors of this series were also tested against the other furin-like PCs and the trypsin-like serine protease thrombin, to examine their selectivity (Table 2).

Compounds **21–26** are also picomolar inhibitors of PC1/3, PC4, PC5/6, and PACE4, although they possess reduced activity against PC7 and are weak PC2 or thrombin inhibitors. It should be noted that all new derivatives shown in Table 2 also have poor potency against the clotting factor Xa and the fibrinolytic enzyme plasmin (data not shown). Nearly all inhibition constants against these proteases were found to be >10 μM, except for inhibitors **24** and **26**, which inhibit plasmin with K_i values of 7.3 and 2.5 μM, respectively. This selectivity profile is similar to that previously reported for inhibitor **1** (34).

Inhibition of HA Cleavage and Influenza Virus Propagation—The infectivity of the influenza virus depends on the correct cleavage of its surface glycoprotein precursor HA0 into the subunits HA1 and HA2. In the case of the highly pathogenic avian influenza subtypes H5 and H7, this processing is performed at a

TABLE 2
Inhibition of furin-like PCs and thrombin by selected inhibitors

No.	K_i							
	hFurin	hPC1/3	mPC4	hPC5/6	hPACE4	hPC7	hPC2	Thrombin
	pM							
1[a]	810	750	ND[b]	1.6×10^3	600	6.2×10^6	3.1×10^5	2.3×10^7
21	70	52	136	69	75	1.2×10^5	$>10^6$	2.5×10^7
22	62	11	68	13	24	9.1×10^4	$>10^6$	1.8×10^6
23	33	ND[b]	24	6.3	30	2.7×10^4	$>10^6$	3.6×10^7
24	16	ND[b]	11.2	1.5	17	2.3×10^4	$>10^6$	1.3×10^7
25	37	44	140	22	74	6.4×10^4	$>10^6$	1.1×10^7
26	8	1.7	23	2.9	5.1	3.2×10^4	$>10^6$	5.9×10^6

[a] The data for inhibitor **1** were included as reference and were taken from a previous publication (34).
[b] It should be noted that K_i values <5 pM were determined for inhibitors **23** and **24** against hPC1/3 based on a single measurement only, due to the limited amount of the enzyme. Therefore, these data are not included in the table.

multibasic cleavage site by furin or PC5/6 during transport of the HA from the endoplasmic reticulum to the plasma membrane. It has been previously suggested that the inhibition of this step might offer a new possibility for antiviral therapy (51, 52). Therefore, we used the furin inhibitors **22** and **24** to investigate their effect on HA cleavage and FPV replication in cell culture. Prior to this, however, we examined the cytotoxicity of these analogs on the viability of the MDCK cells using the 3-(4,5-dimethylthiazol-2-yl)-2,5-diphenyltetrazolium bromide assay (53), because normal virus propagation is possible only in living cells. At concentrations of 25 and 50 μM, inhibitors **22** and **24** were relatively well tolerated by MDCK cells (reduction in cell viability <20% after 24 h and <30% after 48 h). It should be noted that certain other compounds, especially inhibitors **9**, **10**, **11**, and **13**, had a significant cytotoxic effect (see supplemental Fig. S3). Therefore, all analogs with pronounced cytotoxicity were not further investigated in the cell culture experiments.

In a first experiment, we investigated the cleavage of HA (PSKKRKKR ↓ GLFG) in FPV in the presence of different concentrations of inhibitors **22** and **24**. Both derivatives caused a concentration-dependent inhibition of HA processing (Fig. 6). It should be noted that the efficacy of inhibitor **22** is similar to that of the previously described irreversible inhibitor decanoyl-Arg-Val-Lys-Arg-CMK (≈80% inhibition at 50 μM inhibitor concentration), as shown before (34). An improved potency was found for inhibitor **24**, and even at the lowest concentration of 1 μM, it still reduced the HA processing by ~40%. In contrast, we could not detect any beneficial effect with inhibitors modified by various fatty acid residues in a screening experiment (see supplemental Fig. S5). Therefore, these analogs were not further investigated.

Although HA processing is a prerequisite for virus infectivity, the percentage of HA cleavage inhibition provides no clear correlation regarding the amount of remaining infectious virus. Therefore, in an additional experiment the multiple cycle replication of FPV in the presence of inhibitors **22** and **24** was investigated, followed by a microplaque test, which clearly indicates the amount of infectious viruses. Fig. 7 shows the number of released infectious virus particles from MDCK cell cultures at different times over a period of 48 h. Compared with the control lacking inhibitor, both compounds significantly reduced and delayed virus propagation.

The inhibition experiments of multiple cycle replication of FPV were performed over a period of 48 h. Therefore, we also

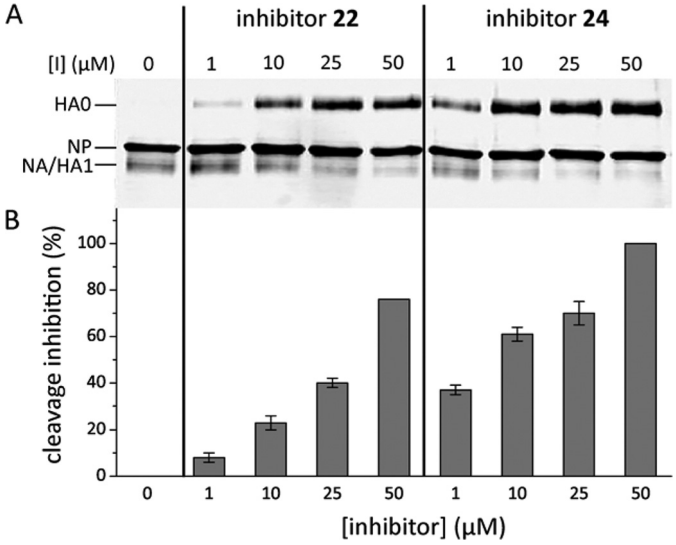

FIGURE 6. **Inhibition of HA cleavage by different concentrations of compounds 22 and 24.** *A,* MDCK cell cultures were infected with FPV at a multiplicity of infection of 100. Inhibition of HA cleavage at different inhibitor concentrations was analyzed 24 h post-infection. Proteins from virus particles (HA0, 82 kDa; nucleoprotein (*NP*), 56 kDa; HA1, 50 kDa; and neuraminidase (*NA*), 50 kDa) were immunochemically detected after SDS-PAGE followed by Western blot analysis. *B,* quantification of HA cleavage inhibition by Western blot analysis ($n = 2$, including S.E.). The maximum amount of HA0, obtained by inhibition with 50 μM of inhibitor **24,** was normalized to 100% cleavage inhibition. Other HA0 band intensities at different concentrations were measured and normalized by standardization of each HA0 value correlating with the corresponding nucleoprotein band. Experimental details are provided in the supplemental material.

determined the stability of both inhibitors in cell culture medium in the presence and absence of MDCK cells by analytical reverse phase HPLC over a period of 96 h. These measurements revealed that both compounds were stable in pure medium, whereas a time-dependent decrease of their concentration was observed in medium containing MDCK cells. After 96 h of incubation, the concentration of inhibitor **24** was reduced by ~30 and 50% when using 30 or 10 μM inhibitor concentrations, respectively (Fig. 8 for inhibitor **24**; data for inhibitor **22** are provided in supplemental Fig. S6). At present, we cannot distinguish whether the concentration decrease in the cell supernatant that we observed is caused by degradation and/or modification of the inhibitors or by cellular uptake, which would presumably be required for the effective inhibition of intracellularly localized furin.

Inhibition of Shiga Toxin Activation—Various toxin-producing bacteria, such as *Shigella dysenteriae* or pathogenic *Esche-*

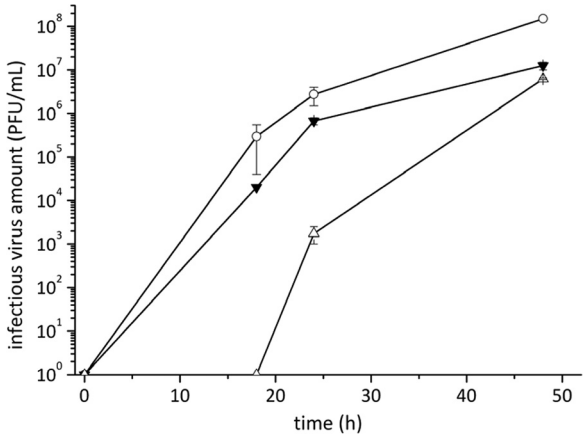

FIGURE 7. **Inhibition of multiple cycle replication of FPV in cell culture in the absence (○) and in the presence of 50 μM of inhibitor 22 (▼) and 24 (△).** Cultures of MDCK cells were inoculated with FPV at a multiplicity of infection of 0.0001. The inhibitor was added to the medium at a final concentration of 50 μM. At different times (0, 18, 24, and 48 h post-infection) the amount of infectious virus (as plaque-forming units (*PFU*) per ml) released into the medium was determined by a microplaque assay (44).

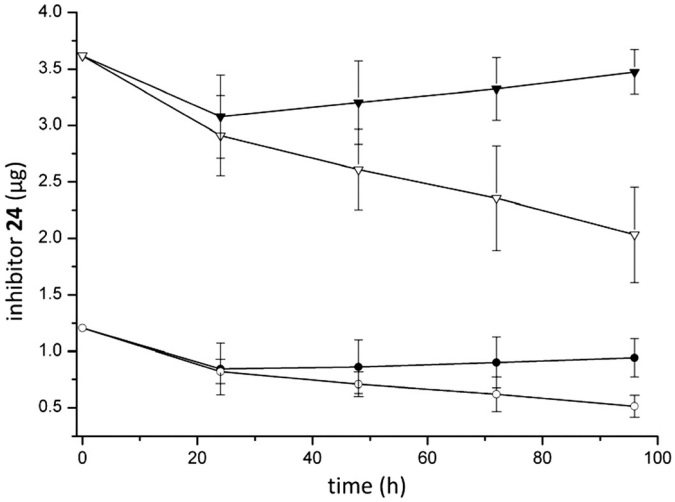

FIGURE 8. **Stability measurements with inhibitor 24 at two different concentrations in pure cell culture medium (30 μM (▼) and 10 μM (●)) and in medium containing MDCK cells (30 μM (▽) and 10 μM (○)).** In all cases, 100 μl of the inhibitor containing medium or supernatant from the cell culture was analyzed by analytical HPLC, which corresponds to ~3.7 μg in the case of the 30 μM solution and to 1.2 μg in the case of the 10 μM solution. The shown data are the mean of two measurements, including S.E.

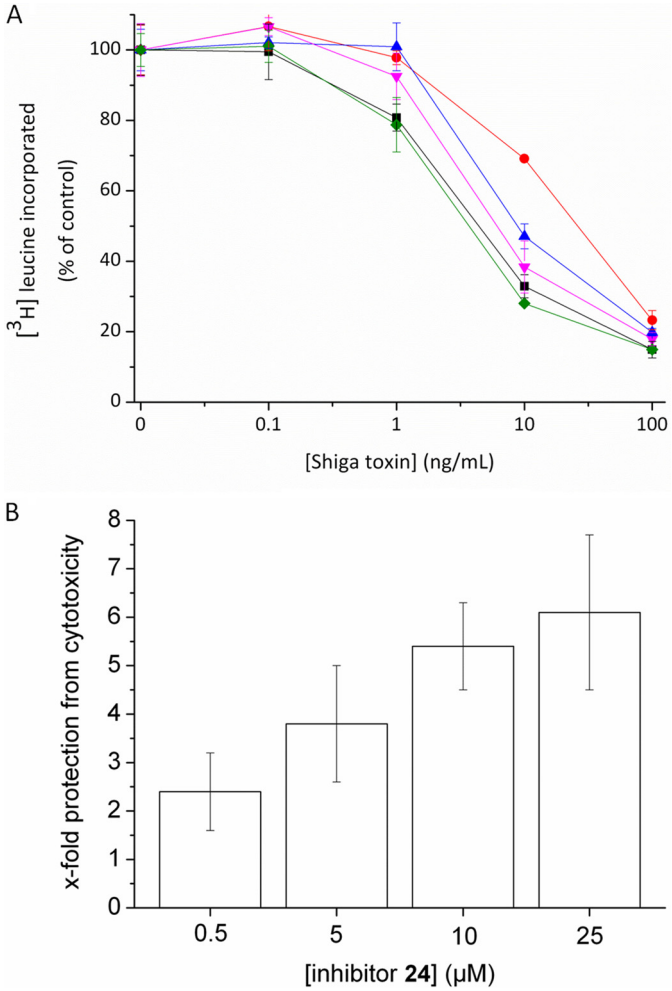

FIGURE 9. **Intoxication of HEp-2 cells by Shiga-toxin (*n* ≥3 for all experiments).** *A*, intoxication was performed in the presence of selected inhibitors (all used at 25 μM; control lacking inhibitor in *black*, ID_{50} 4.4 ng/ml; inhibitor **24** in *red*, ID_{50} 26.1 ng/ml; inhibitor **1** in *blue*, ID_{50} 7.83 ng/ml; Phac-Val-D-Arg-Arg-4-Amba in *magenta*, ID_{50} 6.1 ng/ml; benzylsulfonyl-D-Ser-Lys(Cbz)-4-Amba in *green*, ID_{50} 3.69 ng/ml). *B*, intoxication was performed in presence of various concentrations of inhibitor **24**. No protection was observed at an inhibitor concentration of 0.1 μM.

richia coli strains, can cause serious infections in humans that may lead to diarrhea, hemolytic uremic syndrome, and kidney failure (54). Previous experiments in cell culture revealed that intracellular furin efficiently cleaves the A subunit of the toxin from *S. dysenteriae* into two disulfide-bonded fragments. The thereby activated Shiga toxin has *N*-glycosidase activity that removes a single adenine from the cellular 28 S rRNA of the 60 S ribosomal subunit. This eventually leads to inhibition of protein synthesis in the intoxicated cells (46). Therefore, we tested the ability of inhibitors **1** and **24** to protect HEp-2 cells from intoxication by Shiga toxin. As a control, we used cells lacking inhibitor treatment and cells treated with phenylacetyl-Val-D-Arg-Arg-4-Amba, a structurally closely related analog of inhibitor **1**, which possesses poor furin affinity (see inhibitor **29** in Ref. 35). *In vitro*, activation of Shiga toxin is also possible using trypsin; therefore, the nonspecific trypsin-like serine protease inhibitor benzylsulfonyl-D-Ser-Lys(Cbz)-4-Amba (see inhibitor **33** in Ref. 55), which inhibits trypsin with a K_i value of 5 nM but has negligible affinity against furin, was also included as an additional control. The effect of Shiga toxin on protein synthesis in HEp-2 cells in the absence and presence of these inhibitors is shown in Fig. 9*A*.

In the control lacking added inhibitor, a Shiga toxin concentration of ~4.4 ng/ml was required to reduce cellular protein synthesis by 50% (ID_{50}), whereas ~6-fold higher toxin concentrations were required to achieve this reduction in the presence of inhibitor **24**. A slight protection (1.8-fold) was observed in the presence of compound **1**, whereas negligible efficacy was observed with the poor furin inhibitor phenylacetyl-Val-D-Arg-Arg-4-Amba and the trypsin-like serine protease inhibitor benzylsulfonyl-D-Ser-Lys(Cbz)-4-Amba. It should be noted that additional inhibitors were screened in this assay (data not shown). The irreversible inhibitor Dec-Arg-Val-Lys-Arg-CMK had a slightly reduced protective effect compared with inhibitor

24, whereas only a marginal effect was found for compounds **4**, **6**, and **8**, which were well tolerated by the used HEp-2 cells. In contrast, we observed a very strong cytotoxic effect of inhibitors **9**, **10**, **12**, and **13** modified by longer fatty acid chains in P5 position on HEp-2 cells in the absence of Shiga toxin (see supplemental Fig. S4). Therefore, these inhibitors were not further investigated.

Based on these results, a second experiment with varying concentrations of inhibitor **24** was performed. No protection was observed at 0.1 μM, whereas a concentration-dependent protection was seen at all higher inhibitor concentrations, *e.g.* 5.4-fold ± 0.9 at 10 μM (Fig. 9*B*). These results suggest that inhibitor **24** has a protective effect against intoxication of HEp-2 cells by Shiga toxin, most likely due to inhibition of furin.

DISCUSSION

The implication of furin or furin-like PCs in various diseases is now well established; therefore, efficacious inhibition of these proteases might potentially offer a novel treatment strategy. Although our previously described inhibitors containing a C-terminal 4-amidinobenzylamide (4-Amba) residue had high *in vitro* potency, their efficacy in cell culture as inhibitors of the H7N1 influenza virus propagation was only in the micromolar range, with IC_{50} values around 10 μM. The x-ray structure of furin inhibited by Dec-Arg-Val-Lys-Arg-CMK (36) suggested that the P5 acyl residue might be a suitable position for further optimization of these inhibitors. Because of reports regarding the use of stearylated arginine-rich peptides as efficient transfection systems (56, 57) and experience with the enhanced activity of decanoylated CMK-derived furin inhibitors in cell culture assays, we performed a stepwise prolongation of the P5 acyl chain. Most of the acylated analogs possess a stronger affinity for furin as compared with inhibitor **2** that lacks a P5 residue. This might be explained by interactions found for the P5 carbonyl oxygen in the x-ray complex with the CMK inhibitor (36), which should have a similar backbone conformation compared with our peptidomimetic inhibitors. In the x-ray structure, the decanoyl oxygen binds intramolecularly to one ω-nitrogen of the P4-Arg, which leads to a stabilization of the bound inhibitor conformation and, via a bridging water molecule, to the amide nitrogen of the furin residue Glu-257. It seems reasonable to assume that the elimination of both interactions could reduce the potency of analog **2** by an order of magnitude. Only for longer saturated acyl residues with more than 12 carbon atoms did we observe a gradual decrease in inhibitory activity.

Using light scattering experiments, we could demonstrate that these decreased inhibitory activities might be related to the formation of micelles at concentrations above 0.2 μM. Similar critical micelle formation concentrations in the range of 0.8–0.9 μM were determined for stearylated pentadecapeptides that block sialylgalactose structures on the surface of host cells, which act as receptors for the influenza virus hemagglutinin (58). In this case, the micelles enabled multiple binding and therefore a stronger blockade of the host cell receptors, which resulted in significantly improved inhibition of the virus propagation compared with the nonacylated peptides. In contrast, the saturated C14-C18-furin inhibitors **9–11** exhibit a relatively low inhibitory potency. We surmise that micelles formed by these inhibitors present the inhibitory structures directly on their surfaces. If this is the case, these inhibitors might be less accessible to furin due to steric hindrance. This assumption is supported by results obtained during the design of biotinylated furin inhibitors bound to a streptavidin matrix, which were used for affinity purification. In that case, we observed that specific furin binding required a sufficient linker length between the biotin and the inhibitory moieties (59). A linker length of nine atoms was clearly not long enough, whereas an 18-atom-long linker enabled efficient furin binding. An additional hint for micelle formation as the reason for the reduced potency of the saturated C14-C18 inhibitors was deduced from the incorporation of the linoyl group in inhibitor **14**. This acyl chain contains two *cis*-double bonds and therefore reduces the tendency for micelle formation (Fig. 3). In consequence, inhibitor **14** with an inhibition constant of 5.3 nM possesses an inhibitory potency close to the analogs with shorter acyl groups. However, compounds **14**, **13**, and **11** also reduced the viability of MDCK cells. Therefore, such compounds are not suited for investigations of furin-related processes in cell culture.

Interestingly, despite structural differences, all inhibitors containing a basic P5 residue exhibit improved activity in enzyme kinetic studies. This is quite different from the influence of the basic P4 residue in substrate-analog inhibitors, where only an arginine is accepted, as found previously (35). Replacement by lysine at this site caused an ~350-fold decrease in affinity, which was comparable with that of inhibitors containing a nonbasic citrulline or side chain protected Lys(Cbz) as the P4 residue. Therefore, the improved inhibition constants found for all inhibitors with a basic P5 residue might be partially dependent on faster association of the inhibitors due to a stronger electrostatic binding contribution to the unusually acidic active site of furin. This effect might be comparable with the binding of the highly acidic C-terminal hirudin tail to the basic fibrinogen recognition exosite of thrombin, which contains many Lys and Arg residues. Although it is known from various x-ray structures that several Glu side chains in the C-terminal tail region of hirudin are directed into the solvent and therefore are not involved in direct salt or hydrogen bridges to basic thrombin residues (60), their substitution by glutamine results in weaker thrombin inhibition. Kinetic studies indicated that in all cases where an increase in the dissociation constant (weaker inhibition) was observed, it was predominantly due to a decrease in the association rate constant, whereas the dissociation rate constant was only marginally influenced (61). In contrast, significant differences exist in the inhibitory potency of the furin inhibitors described here, which suggests that the basic P5 groups of the most potent analogs do form specific bonds with furin. Preliminary modeling of inhibitor **26** in complex with furin suggests binding of its P5-guanidino group to the side chain of Glu-230 (supplemental Fig. S7). However, this Glu-230 is relatively solvent-exposed at the furin surface and is not part of a well defined binding pocket.

The most potent compounds **24** or **26** might also be useful tools for convenient active site titration of furin, PC1/3, PC4, PACE4, or PC5/6. Their strong potency leads to significant inhibition at concentrations below that of the enzyme in the assay. A similar approach was described previously for hirudin

titration by thrombin (50) or for thrombin titration by hirudin (62). In general, all analogs tested in this series exhibited low selectivity against other furin-like PCs, such as PC1/3, PC4, PACE4, or PC5/6. Although models of other PCs (63), which are based on the known furin and kexin coordinates, have been built (36, 64, 65), without actual experimental structures it is presently impossible to explain why other PCs, for example PC2 and PC7, are less affected by our inhibitors. The consequences of reduced selectivity of such compounds in practical use are also unknown. A high specificity for the target enzyme would be generally preferred, because it should lead to fewer side effects. However, due to overlapping expression pattern of the PCs, it could perhaps represent an advantage to inhibit more than one PC, to avoid compensation by other PCs in a pathophysiological situation. In contrast, the weak affinity of these analogs for trypsin-like serine proteases is beneficial for the maintenance of blood homeostasis.

The inhibition of host cell proteases such as furin could be a promising approach for the development of new anti-infective drugs. Because a host enzyme is targeted, this strategy would avoid the often-observed emergence of resistance due to mutations in the commonly addressed viral targets. Both inhibitors **22** and **24** caused a significant inhibition in the HA cleavage of a highly pathogenic H7N1 avian influenza strain in virus-infected cell culture assays. Compared with previous results with the reference inhibitor **1** (34), the efficacy of analog **24** was clearly improved; at the lowest concentration of 1 μM, ~35% of the uncleaved HA0 was still maintained. As already discussed, it is impossible to deduce an exact correlation of the extent of HA cleavage inhibition with an effect on virus propagation. More meaningful is the determination of infectious virus particles in a multiple cycle replication assay using a microplaque test. Compared with a control without any inhibitor, only 5% of the amount of infectious virus particles was detected 48 h after treatment with inhibitor **24**. However, animal experiments will be necessary to demonstrate that such delayed virus propagation will result in a beneficial therapeutic effect. Because of their different modes of action, these host cell protease inhibitors could also be useful candidates for combination therapy with already established anti-influenza drugs, for example neuraminidase inhibitors.

In addition to their antiviral effects, furin inhibitors could also represent potential drugs for the treatment of bacterial infections. Various types of furin inhibitors have been used to delay the anthrax toxemia both in cells and in live animals by inhibiting furin-catalyzed processing of the anthrax protective antigen (30, 66, 67). An additional example is the inhibition of the furin-dependent activation of the cytotoxic *Pseudomonas aeruginosa* exotoxin (24, 68). Stimulated by the recent outbreak of enterohemorrhagic *E. coli* infections in Germany, which produce Shiga-like toxins, we tested selected furin inhibitors on their ability to reduce the Shiga toxin activation in cell culture. Inhibitor **24** provided a significant dose-dependent protection against Shiga toxin-induced cytotoxicity in cell culture. However, treatment with inhibitor **24** was unable to afford complete protection against cytotoxicity. This finding is in agreement with earlier studies of cells lacking furin (46) and with studies of mutated Shiga toxins lacking the furin cleavage site (69), suggesting that alternative ways exist, whereby cells can cleave and activate Shiga toxin. It should be noted that furin inhibitor **24** provided no protection against the plant toxin ricin, which has the same effect on ribosomes as Shiga toxin (54), *i.e.* both toxins remove a single adenine from the 28 S RNA of the 60 S ribosome. This demonstrates that inhibitor **24** does not interfere with the similar enzymatic action of these toxins. Therefore, furin seems to be the relevant target for the inhibition of Shiga toxin activation *in vivo*.

In conclusion, we have developed a series of stable and highly potent synthetic furin inhibitors with a relatively broad specificity toward similar PCs, with the exception of PC2 and PC7. Such compounds might be interesting tools for further studies on the physiological role of furin-like PCs and can serve as a starting point for drug development useful for the treatment of furin-related diseases.

REFERENCES

1. Roebroek, A. J., Schalken, J. A., Leunissen, J. A., Onnekink, C., Bloemers, H. P., and Van de Ven, W. J. (1986) Evolutionary conserved close linkage of the c-*fes*/*fps* proto-oncogene and genetic sequences encoding a receptor-like protein. *EMBO J.* **5,** 2197–2202
2. Fuller, R. S., Brake, A. J., and Thorner, J. (1989) Intracellular targeting and structural conservation of a prohormone-processing endoprotease. *Science* **246,** 482–486
3. van de Ven, W. J., Voorberg, J., Fontijn, R., Pannekoek, H., van den Ouweland, A. M., van Duijnhoven, H. L., Roebroek, A. J., and Siezen, R. J. (1990) Furin is a subtilisin-like proprotein processing enzyme in higher eukaryotes. *Mol. Biol. Rep.* **14,** 265–275
4. Steiner, D. F. (1998) The proprotein convertases. *Curr. Opin. Chem. Biol.* **2,** 31–39
5. Seidah, N. G. (2011) What lies ahead for the proprotein convertases? *Ann. N.Y. Acad. Sci.* **1220,** 149–161
6. Schäfer, W., Stroh, A., Berghöfer, S., Seiler, J., Vey, M., Kruse, M. L., Kern, H. F., Klenk, H. D., and Garten, W. (1995) Two independent targeting signals in the cytoplasmic domain determine trans-Golgi network localization and endosomal trafficking of the proprotein convertase furin. *EMBO J.* **14,** 2424–2435
7. Thomas, G. (2002) Furin at the cutting edge. From protein traffic to embryogenesis and disease. *Nat. Rev. Mol. Cell Biol.* **3,** 753–766
8. Plaimauer, B., Mohr, G., Wernhart, W., Himmelspach, M., Dorner, F., and Schlokat, U. (2001) "Shed" furin. Mapping of the cleavage determinants and identification of its C terminus. *Biochem. J.* **354,** 689–695
9. Tian, S., Huang, Q., Fang, Y., and Wu, J. (2011) FurinDB. A database of 20-residue furin cleavage site motifs, substrates, and their associated drugs. *Int. J. Mol. Sci.* **12,** 1060–1065
10. Rockwell, N. C., Krysan, D. J., Komiyama, T., and Fuller, R. S. (2002) Precursor processing by kex2/furin proteases. *Chem. Rev.* **102,** 4525–4548
11. Remacle, A. G., Shiryaev, S. A., Oh, E. S., Cieplak, P., Srinivasan, A., Wei, G., Liddington, R. C., Ratnikov, B. I., Parent, A., Desjardins, R., Day, R., Smith, J. W., Lebl, M., and Strongin, A. Y. (2008) Substrate cleavage analysis of furin and related proprotein convertases. A comparative study. *J. Biol. Chem.* **283,** 20897–20906
12. Roebroek, A. J., Umans, L., Pauli, I. G., Robertson, E. J., van Leuven, F., Van de Ven, W. J., and Constam, D. B. (1998) Failure of ventral closure and axial rotation in embryos lacking the proprotein convertase furin. *Development* **125,** 4863–4876
13. Gu, M., Rappaport, J., and Leppla, S. H. (1995) Furin is important but not essential for the proteolytic maturation of gp160 of HIV-1. *FEBS Lett.* **365,** 95–97
14. Roebroek, A. J., Taylor, N. A., Louagie, E., Pauli, I., Smeijers, L., Snellinx, A., Lauwers, A., Van de Ven, W. J., Hartmann, D., and Creemers, J. W. (2004) Limited redundancy of the proprotein convertase furin in mouse liver. *J. Biol. Chem.* **279,** 53442–53450

15. Creemers, J. W., and Khatib, A. M. (2008) Knock-out mouse models of proprotein convertases. Unique functions or redundancy? *Front. Biosci.* **13,** 4960–4971
16. Fugère, M., and Day, R. (2005) Cutting back on pro-protein convertases. The latest approaches to pharmacological inhibition. *Trends Pharmacol. Sci.* **26,** 294–301
17. Chrétien, M., Seidah, N. G., Basak, A., and Mbikay, M. (2008) Proprotein convertases as therapeutic targets. *Expert Opin. Ther. Targets* **12,** 1289–1300
18. Hallenberger, S., Bosch, V., Angliker, H., Shaw, E., Klenk, H. D., and Garten, W. (1992) Inhibition of furin-mediated cleavage activation of HIV-1 glycoprotein gp160. *Nature* **360,** 358–361
19. Volchkov, V. E., Volchkova, V. A., Ströher, U., Becker, S., Dolnik, O., Cieplik, M., Garten, W., Klenk, H. D., and Feldmann, H. (2000) Proteolytic processing of Marburg virus glycoprotein. *Virology* **268,** 1–6
20. Lahlil, R., Calvo, F., and Khatib, A. M. (2009) The potential anti-tumorigenic and anti-metastatic side of the proprotein convertases inhibitors. *Recent Pat Anticancer Drug Discov.* **4,** 83–91
21. De Vos, L., Declercq, J., Rosas, G. G., Van Damme, B., Roebroek, A., Vermorken, F., Ceuppens, J., van de Ven, W., and Creemers, J. (2008) MMTV cre-mediated for inactivation concomitant with PLAG1 proto-oncogene activation delays salivary gland tumorigenesis in mice. *Int. J. Oncol.* **32,** 1073–1083
22. Garten, W., Stieneke, A., Shaw, E., Wikstrom, P., and Klenk, H. D. (1989) Inhibition of proteolytic activation of influenza virus hemagglutinin by specific peptidyl chloroalkyl ketones. *Virology* **172,** 25–31
23. Basak, A. (2005) Inhibitors of proprotein convertases. *J. Mol. Med.* **83,** 844–855
24. Jean, F., Stella, K., Thomas, L., Liu, G., Xiang, Y., Reason, A. J., and Thomas, G. (1998) α_1-Antitrypsin Portland, a bioengineered serpin highly selective for furin. Application as an antipathogenic agent. *Proc. Natl. Acad. Sci. U.S.A.* **95,** 7293–7298
25. Komiyama, T., and Fuller, R. S. (2000) Engineered eglin c variants inhibit yeast and human proprotein processing proteases, Kex2, and furin. *Biochemistry* **39,** 15156–15165
26. Basak, A., Chen, A., Scamuffa, N., Mohottalage, D., Basak, S., and Khatib, A. M. (2010) Blockade of furin activity and furin-induced tumor cells malignant phenotypes by the chemically synthesized human furin prodomain. *Curr. Med. Chem.* **17,** 2214–2221
27. Angliker, H. (1995) Synthesis of tight binding inhibitors and their action on the proprotein-processing enzyme furin. *J. Med. Chem.* **38,** 4014–4018
28. Basak, A., and Lazure, C. (2003) Synthetic peptides derived from the prosegments of proprotein convertase 1/3 and furin are potent inhibitors of both enzymes. *Biochem. J.* **373,** 231–239
29. Cameron, A., Appel, J., Houghten, R. A., and Lindberg, I. (2000) Polyarginines are potent furin inhibitors. *J. Biol. Chem.* **275,** 36741–36749
30. Kacprzak, M. M., Peinado, J. R., Than, M. E., Appel, J., Henrich, S., Lipkind, G., Houghten, R. A., Bode, W., and Lindberg, I. (2004) Inhibition of furin by polyarginine-containing peptides. Nanomolar inhibition by nona-D-arginine. *J. Biol. Chem.* **279,** 36788–36794
31. Sielaff, F., Than, M. E., Bevec, D., Lindberg, I., and Steinmetzer, T. (2011) New furin inhibitors based on weakly basic amidinohydrazones. *Bioorg. Med. Chem. Lett.* **21,** 836–840
32. Komiyama, T., Coppola, J. M., Larsen, M. J., van Dort, M. E., Ross, B. D., Day, R., Rehemtulla, A., and Fuller, R. S. (2009) Inhibition of furin/proprotein convertase-catalyzed surface and intracellular processing by small molecules. *J. Biol. Chem.* **284,** 15729–15738
33. Jiao, G. S., Cregar, L., Wang, J., Millis, S. Z., Tang, C., O'Malley, S., Johnson, A. T., Sareth, S., Larson, J., and Thomas, G. (2006) Synthetic small molecule furin inhibitors derived from 2,5-dideoxystreptamine. *Proc. Natl. Acad. Sci. U.S.A.* **103,** 19707–19712
34. Becker, G. L., Sielaff, F., Than, M. E., Lindberg, I., Routhier, S., Day, R., Lu, Y., Garten, W., and Steinmetzer, T. (2010) Potent inhibitors of furin and furin-like proprotein convertases containing decarboxylated P1 arginine mimetics. *J. Med. Chem.* **53,** 1067–1075
35. Becker, G. L., Hardes, K., and Steinmetzer, T. (2011) New substrate analog furin inhibitors derived from 4-amidinobenzylamide. *Bioorg. Med. Chem. Lett.* **21,** 4695–4697
36. Henrich, S., Cameron, A., Bourenkov, G. P., Kiefersauer, R., Huber, R., Lindberg, I., Bode, W., and Than, M. E. (2003) The crystal structure of the proprotein processing proteinase furin explains its stringent specificity. *Nat. Struct. Biol.* **10,** 520–526
37. Stieneke-Gröber, A., Vey, M., Angliker, H., Shaw, E., Thomas, G., Roberts, C., Klenk, H. D., and Garten, W. (1992) Influenza virus hemagglutinin with multibasic cleavage site is activated by furin, a subtilisin-like endoprotease. *EMBO J.* **11,** 2407–2414
38. Katayama, S., Hirose, H., Takayama, K., Nakase, I., and Futaki, S. (2011) Acylation of octaarginine. Implication to the use of intracellular delivery vectors. *J. Control Release* **149,** 29–35
39. Bernatowicz, M. S., Wu, Y., and Matsueda, G. R. (1992) 1*H*-Pyrazole-1-carboxamidine hydrochloride an attractive reagent for guanylation of amines and its application to peptide synthesis. *J. Org. Chem.* **57,** 2497–2502
40. Dixon, M. (1953) The determination of enzyme inhibitor constants. *Biochem. J.* **55,** 170–171
41. Williams, J. W., and Morrison, J. F. (1979) The kinetics of reversible tight-binding inhibition. *Methods Enzymol.* **63,** 437–467
42. Bakowsky, H., Richter, T., Kneuer, C., Hoekstra, D., Rothe, U., Bendas, G., Ehrhardt, C., and Bakowsky, U. (2008) Adhesion characteristics and stability assessment of lectin-modified liposomes for site-specific drug delivery. *Biochim. Biophys. Acta* **1778,** 242–249
43. Böttcher-Friebertshäuser, E., Freuer, C., Sielaff, F., Schmidt, S., Eickmann, M., Uhlendorff, J., Steinmetzer, T., Klenk, H. D., and Garten, W. (2010) Cleavage of influenza virus hemagglutinin by airway proteases TMPRSS2 and HAT differs in subcellular localization and susceptibility to protease inhibitors. *J. Virol.* **84,** 5605–5614
44. Matrosovich, M., Matrosovich, T., Garten, W., and Klenk, H. D. (2006) New low viscosity overlay medium for viral plaque assays. *Virol. J.* **3,** 63
45. Kurmanova, A., Llorente, A., Polesskaya, A., Garred, O., Olsnes, S., Kozlov, J., and Sandvig, K. (2007) Structural requirements for furin-induced cleavage and activation of Shiga toxin. *Biochem. Biophys. Res. Commun.* **357,** 144–149
46. Garred, O., van Deurs, B., and Sandvig, K. (1995) Furin-induced cleavage and activation of Shiga toxin. *J. Biol. Chem.* **270,** 10817–10821
47. Jameson, G. W., Roberts, D. V., Adams, R. W., Kyle, W. S., and Elmore, D. T. (1973) Determination of the operational molarity of solutions of bovine α-chymotrypsin, trypsin, thrombin, and factor Xa by spectrofluorometric titration. *Biochem. J.* **131,** 107–117
48. Bender, M. L., Begué-Cantón, M. L., Blakeley, R. L., Brubacher, L. J., Feder, J., Gunter, C. R., Kézdy, F. J., Killheffer, J. V., Jr., Marshall, T. H., Miller, C. G., Roeske, R. W., and Stoops, J. K. (1966) The determination of the concentration of hydrolytic enzyme solutions. α-Chymotrypsin, trypsin, papain, elastase, subtilisin, and acetylcholinesterase. *J. Am. Chem. Soc.* **88,** 5890–5913
49. Bravo, D. A., Gleason, J. B., Sanchez, R. I., Roth, R. A., and Fuller, R. S. (1994) Accurate and efficient cleavage of the human insulin proreceptor by the human proprotein-processing protease furin. Characterization and kinetic parameters using the purified, secreted soluble protease expressed by a recombinant baculovirus. *J. Biol. Chem.* **269,** 25830–25837
50. Stone, S. R., and Hofsteenge, J. (1986) Kinetics of the inhibition of thrombin by hirudin. *Biochemistry* **25,** 4622–4628
51. Garten, W., and Klenk, H. D. (2008) in *Avian Influenza* (Klenk, H. D., Matrosovich, M., and Stech, J., eds) pp. 156–167, S. Karger AG, Basel, Switzerland
52. Garten, W., Hallenberger, S., Ortmann, D., Schäfer, W., Vey, M., Angliker, H., Shaw, E., and Klenk, H. D. (1994) Processing of viral glycoproteins by the subtilisin-like endoprotease furin and its inhibition by specific peptidylchloroalkyl ketones. *Biochimie* **76,** 217–225
53. Mosmann, T. (1983) Rapid colorimetric assay for cellular growth and survival. Application to proliferation and cytotoxicity assays. *J. Immunol. Methods* **65,** 55–63
54. Sandvig, K., Torgersen, M. L., Engedal, N., Skotland, T., and Iversen, T. G. (2010) Protein toxins from plants and bacteria. Probes for intracellular transport and tools in medicine. *FEBS Lett.* **584,** 2626–2634
55. Schweinitz, A., Steinmetzer, T., Banke, I. J., Arlt, M. J., Stürzebecher, A., Schuster, O., Geissler, A., Giersiefen, H., Zeslawska, E., Jacob, U., Krüger,

A., and Stürzebecher, J. (2004) Design of novel and selective inhibitors of urokinase-type plasminogen activator with improved pharmacokinetic properties for use as antimetastatic agents. *J. Biol. Chem.* **279,** 33613–33622

56. Futaki, S., Ohashi, W., Suzuki, T., Niwa, M., Tanaka, S., Ueda, K., Harashima, H., and Sugiura, Y. (2001) Stearylated arginine-rich peptides. A new class of transfection systems. *Bioconjug. Chem.* **12,** 1005–1011
57. Tönges, L., Lingor, P., Egle, R., Dietz, G. P., Fahr, A., and Bähr, M. (2006) Stearylated octaarginine and artificial virus-like particles for transfection of siRNA into primary rat neurons. *RNA* **12,** 1431–1438
58. Matsubara, T., Sumi, M., Kubota, H., Taki, T., Okahata, Y., and Sato, T. (2009) Inhibition of influenza virus infections by sialylgalactose-binding peptides selected from a phage library. *J. Med. Chem.* **52,** 4247–4256
59. Kuester, M., Becker, G. L., Hardes, K., Lindberg, I., Steinmetzer, T., and Than, M. E. (2011) Purification of the proprotein convertase furin by affinity chromatography based on PC-specific inhibitors. *Biol. Chem.* **392,** 973–981
60. Rydel, T. J., Tulinsky, A., Bode, W., and Huber, R. (1991) Refined structure of the hirudin-thrombin complex. *J. Mol. Biol.* **221,** 583–601
61. Braun, P. J., Dennis, S., Hofsteenge, J., and Stone, S. R. (1988) Use of site-directed mutagenesis to investigate the basis for the specificity of hirudin. *Biochemistry* **27,** 6517–6522
62. Dang, Q. D., and Di Cera, E. (1994) A simple activity assay for thrombin and hirudin. *J. Protein Chem.* **13,** 367–373
63. Henrich, S., Lindberg, I., Bode, W., and Than, M. E. (2005) Proprotein convertase models based on the crystal structures of furin and kexin: explanation of their specificity. *J. Mol. Biol.* **345,** 211–227
64. Holyoak, T., Wilson, M. A., Fenn, T. D., Kettner, C. A., Petsko, G. A., Fuller, R. S., and Ringe, D. (2003) 2.4 Å resolution crystal structure of the prototypical hormone-processing protease Kex2 in complex with an Ala-Lys-Arg boronic acid inhibitor. *Biochemistry* **42,** 6709–6718
65. Wheatley, J. L., and Holyoak, T. (2007) Differential P1 arginine and lysine recognition in the prototypical proprotein convertase Kex2. *Proc. Natl. Acad. Sci. U.S.A.* **104,** 6626–6631
66. Sarac, M. S., Peinado, J. R., Leppla, S. H., and Lindberg, I. (2004) Protection against anthrax toxemia by hexa-D-arginine *in vitro* and *in vivo*. *Infect. Immun.* **72,** 602–605
67. Molloy, S. S., Bresnahan, P. A., Leppla, S. H., Klimpel, K. R., and Thomas, G. (1992) Human furin is a calcium-dependent serine endoprotease that recognizes the sequence Arg-*X*-*X*-Arg and efficiently cleaves anthrax toxin protective antigen. *J. Biol. Chem.* **267,** 16396–16402
68. Sarac, M. S., Cameron, A., and Lindberg, I. (2002) The furin inhibitor hexa-D-arginine blocks the activation of *Pseudomonas aeruginosa* exotoxin A *in vivo*. *Infect. Immun.* **70,** 7136–7139
69. Garred, O., Dubinina, E., Holm, P. K., Olsnes, S., van Deurs, B., Kozlov, J. V., and Sandvig, K. (1995) Role of processing and intracellular transport for optimal toxicity of Shiga toxin and toxin mutants. *Exp. Cell Res.* **218,** 39–49